4 Electronic Structure of Condensed Matter

4-1 Observation of Bulk Electronic States of $YBa_2Cu_3O_{7-\delta}$ Using High-Resolution Angle-Resolved Photoemission Spectroscopy

Investigation of low-energy excitations is important in understanding the origin of physical properties such as superconductivity and phase transitions. Previous angle-resolved photoemission spectroscopy (ARPES) studies of the bilayered high-T_c superconductor (HTSC) $Bi_2Sr_2CaCu_2O_{8+\delta}$ (Bi2212) were successful in clarifying several characteristic features, such as a large Fermi surface (FS) centered at the (π, π) point in the Brillouin zone (BZ), an anisotropic $d_{x^2-y^2}$-wave superconducting (SC) gap, and a strong mass renormalization of the band near the Fermi level (E_F) [1, 2]. However, it is still unclear whether or not these characteristic low-energy properties clarified so far for Bi2212 are universal features of HTSCs. In order to address this question $YBa_2Cu_3O_{7-\delta}$ (Y123) is the most suitable candidate for study since it is also a bilayered system with a similar maximum T_c. The electronic structure of Y-based HTSCs has not been well elucidated yet because of the difficulty in distinguishing genuine features of the bulk CuO_2 plane from that of the surface [3-6].

We have performed high-resolution ARPES measurements on untwinned Y123 crystals (nearly optimally-doped, T_c = 92 K) at BL-28A [7]. Clean surfaces for the ARPES studies were obtained by cleaving *in-situ* in an ultrahigh vacuum of 1×10^{-10} Torr.

Figure 1(a) shows the ARPES spectral-intensity as a function of two-dimensional wave vector for Y123 at 10 K. Two distinct hole-like FS sheets (indicated by green lines) are observed, which have their centre at the point marked *S*. A quasi-one-dimensional chain band is also observed (blue line). Figure 1(b) shows ARPES spectral-intensity plots as a function of binding energy and wave vector at four representative cuts (labelled A-D) of the plot of Fig. 1(a). Along *cut A*, two bands corresponding to the two FS sheets shown in Fig. 1(a) can be seen. These bands clearly cross E_F, showing that the crystal displays metallic nature even at a temperature well below the bulk T_c. These bands therefore do not reflect the bulk superconductivity, and are assigned as bonding and antibonding bands derived from the cleaved topmost CuO_2 bilayer. We have estimated the hole concentration (x) from the volume of the bonding and antibonding FSs to be x = 0.29 ± 0.02, which corresponds to the doping level at the boundary between the SC and the metallic phase in the heavily overdoped

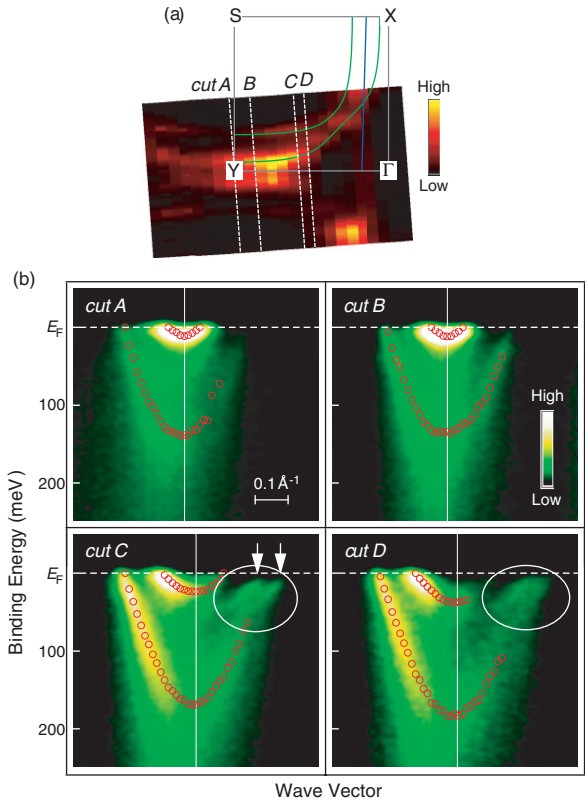

Figure 1
(a) ARPES spectral-intensity as a function of two-dimensional wave vector recorded at 10 K for the Y123 E_F using 46-eV photons. The ARPES intensity is integrated over an energy range of 30 meV centered at E_F. The green and blue lines are guides for the eyes as to the location of the FSs. (b) ARPES intensity plots as a function of binding energy and wave vector along several cuts shown by the white lines in (a). The peak positions in the ARPES spectra for the surface bands after eliminating the effect of the Fermi-Dirac distribution function are shown by open red circles. White arrows represent the positions of k_F points for the bulk bands.

region. These surface bands show an asymmetric intensity variation with respect to the ΓY high symmetry line (the solid white line in Fig. 1b), indicating a strong matrix-element effect due to the circular polarization of the incident light. In addition to the surface bands, we can unambiguously identify another feature near E_F in the momentum location where the spectral intensity of the surface bands is significantly suppressed (the area enclosed by a white circle in the plots for cuts C and D). As is clearly visible in the plot for *cut C*, this feature consists at 10 K of two independent bands showing a finite gap. A similar feature is also observed in *cut D* although the spectral feature is relatively vague. We assign this gapped pair of bands as the bonding and antibonding bands which originate in the bulk CuO_2 plane.

By reducing the contribution from the surface band by tuning the photon energy and the polarization, we have determined the detailed momentum dependence of the SC gap in Y123 for the first time. Figure 2(a)

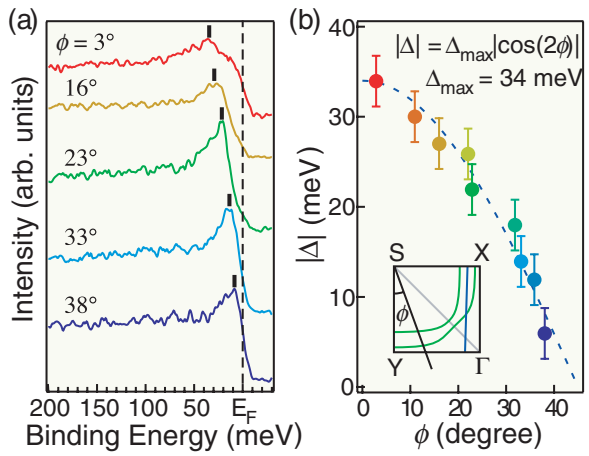

Figure 2
(a) ARPES spectra recorded at 10 K for various k_F points of the bulk bands. (b) Momentum dependence of the SC-gap size (Δ) as a function of FS angle (ϕ, defined in the inset). The dashed line represents the best fit using the $d_{x^2-y^2}$-wave gap function.

shows ARPES spectra recorded at 10 K for various k_F points of the bulk bands characterized by the FS angle (ϕ) defined in the inset to Fig. 2(b). We clearly find a sharp superconducting coherence peak which shows a significant momentum dependence, reflecting the anisotropic superconducting-gap opening. The obtained *k*-dependence of superconducting gap (Δ) is shown in Fig. 2(b). This Δ is strongly *k*-dependent and gradually becomes small as ϕ approaches 45°, revealing itself as a $d_{x^2-y^2}$-like order parameter, as observed in previous ARPES studies on Bi2212. The present ARPES results unambiguously demonstrate the universality of bulk electronic states in bilayered HTSCs and open a way to systematic ARPES investigations of Y-based HTSCs.

K. Nakayama[1], T. Sato[1], K. Terashima[1], H. Matsui[1], T. Takahashi[1], M. Kubota[2], K. Ono[2], T. Nishizaki[1], Y. Takahashi[1] and N. Kobayashi[1] ([1]Tohoku Univ., [2]KEK-PF)

References

[1] A. Damascelli, Z. Hussain and Z.-X. Shen, *Rev. Mod. Phys.*, **75** (2003) 473.
[2] J.C. Campuzano, *et al.*, *The physics of Superconductors,* edited by K. H. Bennemann, J. B. Bennemann and J. B. Ketterson (Springer, New York, 2003).
[3] J.G. Tobin, C.G. Olson, C.Gu, J.Z. Liu, F.R. Solal, M.J. Fluss, R.H. Howell, J.C. O'Brien, H.B. Radousky and P.A. Sterne, *Phys. Rev. B*, **45** (1992) 5563.
[4] M.C. Schabel, C.-H. Park, A. Matsuura, Z.-X. Shen, D.A. Bonn, R.Liang and W.N. Hardy, *Phys. Rev. B*, **57** (1998) 6090.
[5] M.C. Schabel, C.-H. Park, A. Matsuura, Z.-X. Shen, D.A. Bonn, R. Liang and W.N. Hardy, *Phys. Rev. B*, **57** (1998) 6107.
[6] D.H. Lu, D.L. Feng, N.P. Armitage, K.M. Shen, A. Damascelli, C. Kim, F. Ronning, Z.-X. Shen, D.A. Bonn, R. Liang, W.N. Hardy, A.L. Rykov and S. Tajima, *Phys. Rev. Lett.*, **86** (2001) 4370.
[7] K. Nakayama, T. Sato, K. Terashima, H. Matsui, T. Takahashi, M. Kubota, K. Ono, T. Nishizaki, Y. Takahashi and N. Kobayashi, *Phys. Rev. B*, **75** (2007) 014513.

4-2 Anomalous Electronic Correlations in the Momentum Density of $Al_{97}Li_3$

Random disordered Al-Li alloys, which are well-known hard materials with a high strength to weight ratio, have been developed empirically in the aircraft industry and related fields without thorough understanding of the electronic structure of these alloys. Often they exhibit a property unexpected from their constituent atoms which are commonly thought of as being a free-electron-like metal.

In this study we report that the electron momentum density in $Al_{97}Li_3$ differs significantly from the prediction of the conventional Fermi-liquid picture and that the electronic ground state of Al is modified anomalously by the addition of Li atoms of just a few percent [1].

To directly probe changes in the electronic ground state of Al due to the presence of Li atoms, we employed Compton scattering measurements. Compton scattering is one of a few methods that can directly probe the bulk electronic ground state in materials. The measured double differential cross-section, usually referred to as the Compton profile, is given by

$$J(p_z) = \iint \rho(\boldsymbol{p}) dp_x dp_y \quad , \qquad (1)$$

where $\rho(\boldsymbol{p})$ is the ground-state electron momentum density and p_z is taken along the X-ray scattering vector. The theoretical analysis of the Compton profile is often based on the expression of $\rho(\boldsymbol{p})$ within the independent particle model. For a random disordered alloy, the ensemble averaged momentum density can be obtained by the first-principles Korringa-Kohn-Rostoker coherent potential (KKR-CPA) framework within the local density approximation (LDA) [2].

With regard to the experiment, a single crystal of $Al_{97}Li_3$ was grown by the Bridgman method, and the Compton profiles were measured along the [100], [110] and [111] directions with a momentum resolution of 0.12 atomic units (a.u.) by the high-resolution Compton scattering spectrometer installed at AR-NE1A1. The Compton profiles of Al used for comparison were measured by Ohata *et al.* [3] under the experimental conditions of the present measurements. Concerning computation of the corresponding theoretical profiles, self-consistent electronic structures were first obtained for $Al_{1-x}Li_x$ at x = 0 and 0.03, respectively using the KKR-LDA-CPA scheme. These results were used to evaluate $\rho(\boldsymbol{p})$.

We consider the measured and computed changes in the Compton profiles of the valence electrons,

$$\Delta J(p_z) = J(p_z)_{Al} - J(p_z)_{Al_{97}Li_3}. \qquad (2)$$

Further, to make our discussion brief and to the point, we consider the spherical average ΔJ_{sph} of the change ΔJ. Figure 3 presents the results for ΔJ_{sph}. The theoretical KKR-CPA curve (blue dashed line) differs substantially from the experimental data (red dots).

Note that correlation effects of the standard homogeneous electron gas are present in $Al_{97}Li_3$ with a magnitude similar to that of Al because the electron density in Al and $Al_{97}Li_3$ is nearly the same, with the Fermi momentum p_F (about 0.92 a.u.) differing by only about 1%. Therefore, the substantial discrepancy shown in Fig. 3 cannot be explained by the standard electron gas theory. The key to understand this discrepancy is to recognize that correlation effects can be viewed as exciting some electrons into higher energy unoccupied orbitals as a way of modifying the character of the ground-state wave-function. The lowest unoccupied orbitals in Li and Al are the 2*p* and 3*p* orbitals. It is natural to consider the effect of promoting an electron from an *s* to a *p* orbital. The resulting change in the Compton profile can be straightforwardly computed as described in Ref. [1]. The green solid line in Fig. 3 shows the result of correcting the KKR-CPA ΔJ_{sph} by promoting 3% valence electrons in $Al_{97}Li_3$ from *s*- to *p*-like states. We may look upon this result as indicating that correlations and the associated changes in the effective potentials produce an enhanced *p* character of the ground state wave-function of $Al_{97}Li_3$. Note that since only 1% of valence electrons in $Al_{97}Li_3$ come from Li atoms, the promotion needed indicates a significant involvement of Al electrons near the Li impurities in generating the anomalous changes in the momentum density of the alloy. This work was partially supported by U.S. D.O.E. Contract No. DE-AC03-76SF00098 and by the Polish Committee for Scientific Research No. 2 P03B 028 14.

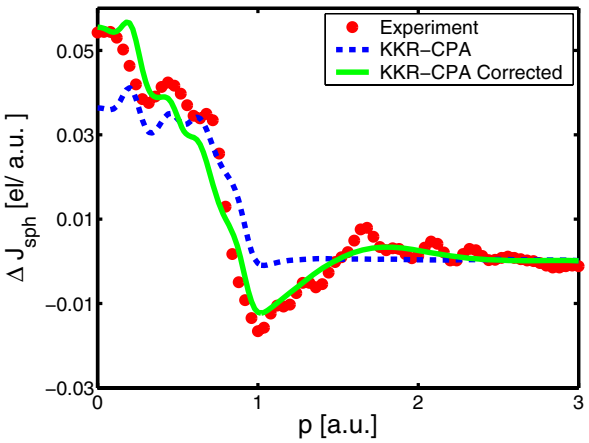

Figure 3
Spherical average of experimental ΔJ defined in eq. (1) is compared with the corresponding KKR-CPA result with and without the correction.

J. Kwiatkowska[1], B. Barbiellini[2], S. Kaprzyk[2, 3], A. Bansil[2], H. Kawata[4] and N. Shiotani[4] ([1]H. Niewodniczanski Inst. Nucl. Phys., [2]Northeastern Univ., [3]AGH Univ. Sci. & Tech., [4]KEK-PF)

References

[1] J. Kwiatkowska, B. Barbiellini, S. Kaprzyk, A. Bansil, H. Kawata and N. Shiotani, *Phys. Rev. Lett.*, **96** (2006) 186403.

[2] A. Bansil, B. Barbiellini, S. Kaprzyk and P.E. Mijnarends, *J. Phys. Chem. Solids*, **62** (2001) 2191.

[3] T. Ohata, M. Itou, I. Matsumoto, Y. Sakurai, H. Kawata, N. Shiotani, S. Kaprzyk, P.E. Mijnarends and A. Bansil, *Phys. Rev. B*, **62** (2000) 16528.